DYNA
http://dyna.medellin.unal.edu.co/

UNIVERSIDAD NACIONAL DE COLOMBIA

Susceptibility to moisture damage in asphalt mixes with blast furnace dust as aggregate

Ricardo Ochoa-Díaz [a], Gloria Elizabeth Grimaldo-León [b] & Carlos Hernando Higuera-Sandoval [a]

[a] *Grupo de Investigación y Desarrollo en Infraestructura Vial, Universidad Pedagógica y Tecnológica de Colombia, Tunja, Colombia. ricardo.ochoa@uptc.edu.co, carlos.higuera@uptc.edu.co*
[b] *Grupo de Investigación en Logística, Operaciones, Gestión y Calidad, Universidad de Boyacá, Tunja, Colombia. gegrimaldo@uniboyaca.edu.co*

Received: January 31th, 2024. Received in revised form: May 29th, 2024. Accepted: June 7th, 2024.

Abstract
One of the ongoing challenges in engineering is mitigating the degradation of road infrastructure caused by water in asphalt mixes. This study aims to assess the impact of blast furnace dust, a byproduct of the steel manufacturing process, on moisture-induced damage in asphalt mixes. Three asphalt mixes were developed following the Marshall methodology: one comprising conventional crushed aggregates, while the others substituted 50% and 100% of the conventional fine aggregate with blast furnace dust. Material characterization procedures and chemical analysis of the blast furnace dust were conducted. Once compliance with the specified material requirements was verified and analyzed, water susceptibility was evaluated through an indirect tensile test across various void content levels. Similarly, leveraging the Superpave gyratory compactor, several compaction indices were determined to estimate the compaction behavior of each mix. Based on the findings, the inclusion of blast furnace dust in an asphalt mix proved satisfactory due to its contributions in enhancing tensile strength, consequently leading to a reduction in moisture-induced damage within the asphalt mix, as well as exhibiting improved compaction behavior. Additionally, this utilization contributed to diminishing the environmental impact linked to the steel production process, where substantial quantities of this residue accumulate.

Keywords: asphalt mixture; blast furnace dust; energy of compaction; moisture susceptibility; recycling.

Susceptibilidad al daño por humedad en mezclas asfálticas con polvo de alto horno como agregado

Resumen
Uno de los desafíos constantes que enfrenta la ingeniería es reducir el deterioro de la infraestructura vial debido al agua en las mezclas asfálticas. La presente investigación busca evaluar la incidencia del polvo de horno alto, un subproducto del proceso del acero, en el daño por humedad en las mezclas asfálticas. Se diseñaron tres mezclas asfálticas bajo la metodología Marshall: una está compuesta por agregados convencionales triturados, las otras sustituyendo el 50% y 100% del agregado fino convencional por polvo de horno alto. Se llevaron a cabo los procedimientos de caracterización de materiales respectivos y la caracterización química del polvo de horno alto. Una vez verificado y analizado el cumplimiento de los requisitos establecidos para los materiales, se evaluó la susceptibilidad al agua utilizando una prueba de tracción indirecta para diferentes contenidos de vacíos. Del mismo modo, y aprovechando el compactador giratorio Superpave, se determinaron algunos índices de compactación y así se estimó el comportamiento de compactación de cada mezcla. Basándose en los resultados, el uso del polvo de horno alto en una mezcla asfáltica es satisfactorio debido a sus contribuciones para mejorar la resistencia a la tracción, lo que resultó en una reducción del daño por humedad en la mezcla asfáltica, así como un mejor comportamiento en la compactación. Además, se contribuyó a reducir el impacto ambiental causado por el proceso del acero, donde se acumulan grandes cantidades de este residuo.

Palabras clave: mezcla asfáltica; polvo de alto horno; energía de compactación; susceptibilidad a la humedad; reciclaje.

1 Introduction

The integral steelmaking process starts from exploiting raw materials: limestone, coal and, of course, iron ore. These materials reach primary manufacturing and undergo their first transformation. Coal is distilled in the coking plant to convert it into coke; the fines (iron, limestone, and coke) are transformed to a suitable granulometry in the sinter plant, and

How to cite: Ochoa-Díaz, R., Grimaldo-León, G.E., and Higuera-Sandoval, C.H., Susceptibility to moisture damage in asphalt mixes with blast furnace dust as aggregate. DYNA, 91(232), pp. 149-158, April - June, 2024..

all the materials for the manufacture of pig iron are melted in the blast furnace. Next, the pig iron is transformed into steel, and the rolling phase transforms the steel into the final finished product.

Throughout the process, waste is generated; in the case of the blast furnace, dust, sludge and slag. Blast furnace slag (BFS) is generated by the segregation of impurities and is composed of calcium, aluminum, silicates, and oxides of silicon and magnesium [1]. Blast furnace dust (BFD) is a waste with very little use; it contains iron, carbon and low amounts of magnesium, silicon, aluminum and calcium [2]. BFD is produced during the cleaning of gases produced in the manufacture of pig iron. The approximate production of BFD is from 7 to 45 kg per ton of pig iron [1].

Today, sustainability and environmental factors are important in pavement production and construction, and materials have come under investigation. Therefore, research regarding BFD as a partial or complete substitute for fine aggregate in an asphalt mix, and evaluation of damage by humidity, is proposed.

One of the most frequent damages in asphalt pavements is caused by the effect of water, especially in high rainfall areas [3]. This phenomenon is associated with the asphalt cement's cohesion, and the adhesion between the aggregate and the asphalt cement [4]. To somewhat mitigate this problem, it is necessary to look for alternative materials that improve the performance of asphalt mixes.

Our result analysis follows the different stages of this research. The first part included the physical characterization of the materials used: stone aggregates, blast furnace dust and asphalt cement. Second, BFD components and texture were identified. Lastly, the dosage of the materials, the design process for the proposed mixtures and the performance of the susceptibility test to humidity damage for different percentages of voids were reviewed.

Figure 1. Blast furmace dust
Source: the authors.

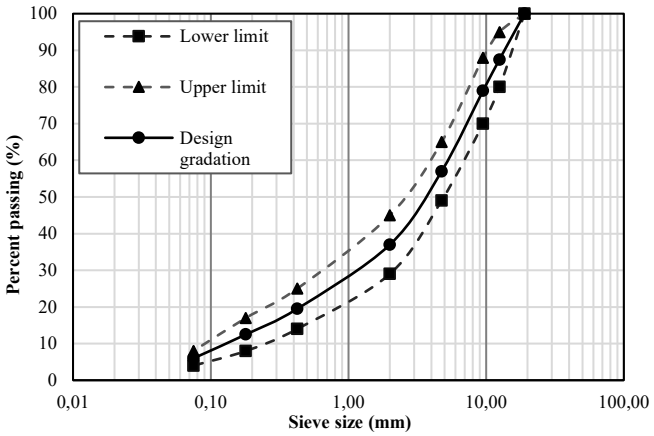

Figure 2. Working gradation for mixtures type MCD-19 according to article 450-13 INVIAS
Source: the authors.

2 Materials and methodology

Mixture design was carried out under the Marshall method with its specific procedures. Three asphalt mixes were designed: the first (M-0) was made with conventional natural aggregates (gravel and sand); in the second (M-50), 50% of the fine aggregate was replaced by BFD; and in the third (M-100), 100% of its fine aggregate was replaced by BFD. The Superpave Gyratory Compactor was used for compaction.

2.1 Materials

Two companies located in the department of Boyacá (Colombia) supplied the research materials. Triturados Paz de Río supplied the natural stone materials, and the steel company Votorantim-Paz de Río S.A. provided the BFD, Fig. 1. As a binder, 80-100 penetration asphalt cement was used according to the classification of Article 410-13 of the general road construction specifications INVIAS [5]. The physical and mechanical properties of the aggregates and asphalt cement are shown in Tables 1 and 2. Mixtures were designed under the grading curve of a hot-dense mix MDC-19, Fig. 2 for research analysis [6].

The BFD was included in the granulometry in the range of passing sieve No. 4 and retained on sieve No. 200. This distribution maintains the sizes for the MDC-19 mix. The dosage of the aggregates was sampled by volume for the different mixtures, and the dosage of the asphalt binder was sampled by weight [7], accounting for the difference in mass between the sand and the BFD.

The X-ray fluorescence (XRF) technique was performed using a Rigaku Primus II sequential spectrometer with a rhodium tube and a 30-micron beryllium window to know the BFD's chemical composition. Likewise, to know the BFD phases, X-ray diffraction (XRD) analysis was performed. The test was carried out with the Panalytical equipment, model Empyrean, equipped with a copper tube, using the Bragg - Brentano optical configuration, and with a high-speed, solid-state detector for data acquisition called PIXEL 3D 2x2. We worked at an acceleration voltage of 45 kV, a current intensity of 40 mA, and with a sweep angle (2θ) from 6.0996° to 81.98096°. This test is based on the relationship between the intensities of the diffraction peaks of a defined mineralogical phase. Fig. 3 shows the XRD spectrum of the BFD used in the investigation.

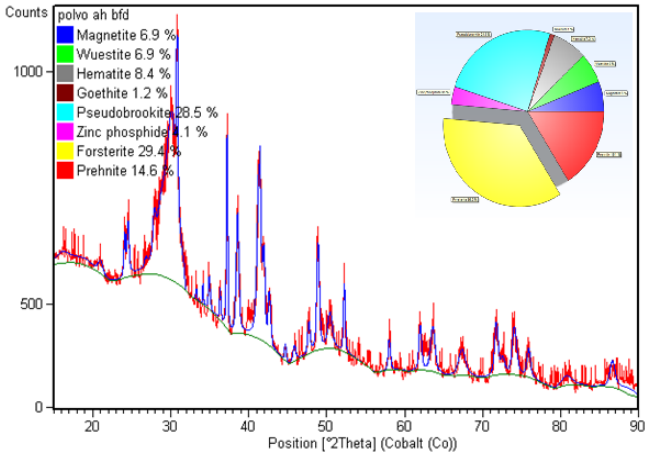

Figure 3. XRD spectrum result of the tested BFD
Source: the authors.

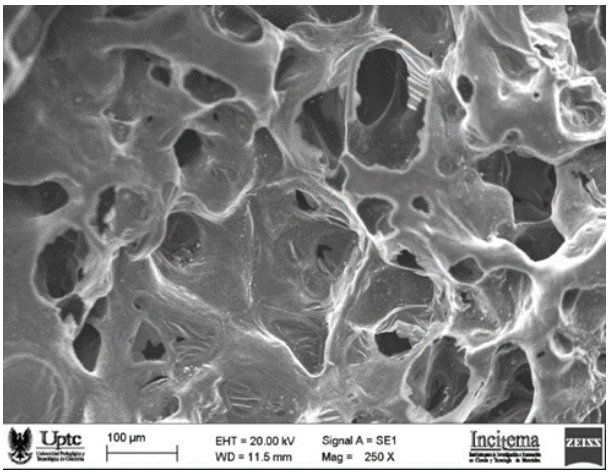

Figure 4. SEM micrograph of the BFD
Source: the authors.

In addition, the BFD particles were subjected to microscopic examination to characterize their shape and surface texture. The examination was performed with the Leo 410 scanning electron microscope (SEM), with a chamber vacuum of 9.85E-5 Torr, filament current of 1.2 nA, and anode voltage of 15 kV.

Fig. 4 presents an SEM micrograph of BFD at a scale of 250X, which presents pores and a rough texture with rounded edges. A strong adhesion bond with asphalt cement can be attributed to these characteristics of texture and roughness [8-9].

BFD analysis shows compounds rich in iron and magnesium. The BFD had iron hydroxides ($Fe(OH)_2$), evidencing water exposure with its ongoing reaction. There are also forsterite-type magnesium silicates (Mg2SiO4) generated at high temperatures, which present calcium and aluminum silicates such as prehnite ($Ca_2Al(Si_3Al)O_{10}(OH)_2$), Goethite ($\alpha$-$Fe_3$+O(OH)) which is formed under oxidizing conditions as a product of the weathering of iron-bearing minerals.

According to Table 3, BFD's main chemical component is Fe_2O_3 with 77.50%, followed by SiO_2 (5.50%), and CaO (4.95%). In the sand, as expected, the main component is SiO_2 at 88.70%, Fe_2O_3 at only 0.99%, and CaO at 0.46%. In the gravel-type coarse aggregate, the main constituents are CaO (63.40%), SiO_2 (16.60%), and Al_2O_3 (9.30%). Regarding the BFD's volumetric expansion, it can be asserted that this material has a low probability of having expansive characteristics due to the low content of CaO and MgO [10-12].

Table 1.
Basic physical properties of the aggregates used

Test	BFD			Specification	Standard
	Course	Fine	Fine		
Loss Angeles Abrasion (%)	20	-	-	<25	ASTM C 131
Degradation (Micro-Deval) (%)	19.4	-	-	<25	ASTM D 6928
Mechanical strength, 10% fine (kN)	122.7	-	-	>110	SABS Meth 842
Fractured particles (%)	94.1	-	-	>85	ASTM D 5821
Plasticity index (%)	-	NP	NP	NP	ASTM D 4318
Sand equivalent (%)	-	70	93.8	>50	ASTM D 2919
Bulk specific gravity	2.62	2.71	2.36	-	ASTM C 127/128
Absorption (%)	1.2	3.1	5.6	-	

Source: The authors

Table 2.
Basic properties of asphalt cement

Properties	Measured values	Specification	Standard
Penetration at 25°C (0.1 mm)	83.5	80 - 100	ASTM D 5-97
Ductility, 5 cm/min, 25°C (cm)	102	>100	ASTM D 113
Softening point (°C)	46.0	>45	ASTM D 36
Flashpoint (°C)	266	>230	ASTM D 92
Viscosity at 60°C (P)	1490	>1000	ASTM D 2171

Source: The authors

Table 3.
Chemical composition of aggregates in XRF

Component	Gravel	Sand	BFD
	% in weight		
MgO	3.80	1.60	1.00
Al_2O_3	9.30	7.30	3.60
SiO_2	16.60	88.70	5.50
P_2O_5	-	-	0.20
CaO	63.40	0.46	4.95
MnO	0.17	-	3.32
Fe_2O_3	3.04	0.99	77.50
Others	3.63	1.00	0.90

Source: The authors

The CaO/SiO_2 ratio establishes the alkalinity level of the material. Alkalinity is classified into three grades [13]: low (<1.8), intermediate (1.8-2.5), and high (>2.5) alkalinity. Intermediate or high alkalinities define a good affinity between the aggregate and the asphalt binder [14][15]. The coarse aggregate presents a ratio of 3.8, which indicates a good affinity. The BFD's CaO/SiO_2 ratio is 0.9; in the sand, it is 0.005. Therefore, BFD has a better affinity with asphalt cement.

It is not imperative that the results obtained through XRF and XRD analyzes necessarily coincide. These techniques provide different perspectives on the sample and rely on different principles to obtain their data. While XRF is used to identify the elemental composition of the sample and quantify the concentration of the elements present, XRD is used to reveal the crystal structure of the sample.

The XRF data support the presence of Fe_2O_3 identified by XRD as iron hydroxides and goethite. The XRF data also indicate the presence of other elements such as SiO_2, CaO and Al_2O_3, which are consistent with the silicates, calcium and aluminum identified by XRD. The XRD and XRF results provide complementary and coherent information about the BFD material, supporting the presence of specific compounds and their chemical composition.

2.2 Methodology

2.2.1 Compaction indices

The Superpave gyratory compactor (SGC) is a laboratory device that simulates the compaction process on a large scale, considering factors such as temperature, density, and stiffness. This allows for a more accurate measurement of compaction and a more consistent production of high-quality asphalt mixes.

Considering that, in this investigation the specimens were compacted with the SGC, the compaction curves were drawn, depending on the voids with air (%Av) and the percentage of the theoretical maximum specific gravity (%G_{mm}) against the number of turns. (N). Since the voids with air and the level of compaction influence the behavior of the asphalt mix, the studied mixes were analyzed, calculating the following indices:

Compaction energy index (CEI)

The compaction energy index (CEI) is the area under the compaction curve (number of gyrations Vs. % G_{mm}) from gyration number eight to the gyration in which 92% of G_{mm} is reached, as shown in Figure 5 (in the Results and Discussion section to follow), which represents the compaction carried out during the construction of the asphalt folder. It is taken from gyration eight to simulate the compaction carried out by the paver during the process of spreading the mix, and 92% of G_{mm} is the approximate density (Av = 8%) at the end of the construction process and giving the service to the transit [16]. The CEI can be calculated with eq. (1)[17].

$$CEI = \sum_{N=8}^{N\ 92\%} \%G_{mm} \quad (1)$$

Where:
CEI = compaction energy index
N92% = number of gyrations 92% of maximum theorical density
%G_{mm} = percent of maximum theorical density.

Traffic compaction index (TCI)

This index is defined as the area under the compaction curve (number of gyrations Vs. % G_{mm}) from 92% of G_{mm} through 96% of G_{mm} (Av=4%) [16][18] and up to the end of the compaction curve in Figure 5. The pavement continues to compact under vehicle loads, and, according to construction and design specifications, it is required that the mix be compacted to 96% G_{mm} (Av = 4%). The TCI evaluates the compaction to which the mix is subjected after the pavement is put into service and that is caused by the loads of the vehicles. The TCI is calculated with eq. (2) [17].

$$TCI = \sum_{N\ 92\%}^{N96\%\ y\ End\ cc} \%G_{mm} \quad (2)$$

Where:
TCI = traffic compaction Index
N92% = number of gyrations 92% of maximum theorical density
N96% = number of gyrations 96% of maximum theorical density and maximum compaction
%G_{mm} = percent of maximum theorical density.

Mix stability index (MSI)

This index is defined as the area under the compaction curve (number of gyrations Vs. % Air Voids) from turn number eight to the turn in which 8% Air voids in the mix is reached (92% of G_{mm}) [19] as shown in Figure 6 (In the Results and Discussion section to follow). This index indicates the energy used in the compaction process of the asphalt layer during construction. Av = 8% is used, considering that during the construction process the mixture will remain with that percentage of voids (92% of the G_{mm}). The MSI is calculated with eq. (3) [17].

$$MSI = \sum_{N=8}^{N\ 8\%\ Av} \%Av \quad (3)$$

Where:
MSI = mix stability index

N8% Av= number of gyrations 8% of air voids
%Av = Air voids.

Mix resistance index (MRI)

The mix resistance Index is the area under the compaction curve (number of gyrations vs. % Air Voids) from the gyrations where 8% air voids are reached (Air Voids after the construction process is finished) passing through the gyrations where 4% Air Voids are reached and up to the end of the compaction curve [19] as seen in Figure 6. This index indicates the ability to withstand compaction under the action of vehicle loads during the pavement's service life. The MRI is calculated using eq. (4) [17].

$$MRI = \sum_{N8\%\ Av}^{N\ 4\%\ Av\ y\ end\ CC} \%Av \quad (4)$$

Where:
MSI = Mix resistance index
N8%Av = number of gyrations 8% of Air Voids,
N4% = number of gyrations 4% of Air Voids and maximum compaction
%Av = Air Voids.

In this study the compaction indices were determined for the different percentages of Air voids. That is, 4, 6, 8 and 10% (96, 94, 92 and 90 % G_{mm}).

2.2.2 Moisture damage susceptibility test

Various methods are found in the literature to assess how susceptible an asphalt mix is in the presence of water. In this study, the tensile strength ratio (TSR) method was used, for which the description in the ASTM D4867/D4867M-96 standard was considered, and which consisted of the preparation of six Marshall-type cylindrical specimens for each type of mixture, which are compacted until obtaining a percentage of air voids of 7±1%. The test tubes produced are divided into two groups: a group of three test tubes are conditioned (as defined below), and the other group is kept dry throughout the test process. Conditioning consists of bringing the specimens to partial saturation until obtaining a saturation between 55% and 80%. Finally, before the tensile specimens fail, all the specimens are placed in a water bath at 25 ℃ for two hours [20].

In accordance with the standards, the test is carried out at a controlled deformation rate at a load speed of 50 mm/min (2 in./min). The average tensile strength of the conditioned specimens (Stm) is compared with the average tensile strength of the unconditioned specimens (Std). The tensile strength in each case is calculated with eq. (5), and the resistance ratio (TSR) between the conditioned and unconditioned specimens is expressed with eq. (6).

$$S_t = \frac{2000 * P}{\pi * t * D} \quad (5)$$

$$TSR = \frac{S_{tm}}{S_{td}} * 100 \quad (6)$$

Where:
St = tensile strength in kPa
P = maximum load in N
t = specimen thickness in mm
D = specimen diameter in mm.

In this study and to evaluate the incidence of BFD as a fine aggregate in asphalt mixes, the test was carried out with groups of specimens and with a variation of the percentage of voids of air with 4%, 6%, 8%, and 10% in each type of mix.

3 Results and discussions

3.1 Design of the mixtures

3.1.1 Preliminary design

Table 4 contains the Marshall design parameters for each mixture. There was a variation in the optimum asphalt content; in the base mix M-0, it was 5.4%, and in the mixes with BFD, they were 7.2% for mix M-50 and 7.9% for mix M-100. This increase can be attributed to the characteristics of shape and texture found in the BFD and the percentage of absorption found for this material.

The stabilities for mixtures M-0, M-50 and M-100 were 13,500 N, 12,100 N, and 11,200 N, respectively, which met the requirements specified. M-50, made by substituting 50% of the fine aggregate with BFD, presented a 10% lower stability concerning the base mix but 34% higher concerning the minimum specified stability. M-100, made by substituting 100% of the fine aggregate with BFD, was the least stable of the mixes, yet still 24% higher than the minimum required. The decreased stability of these mixtures can be attributed to the higher asphalt cement content since a thicker asphalt cement film appears surrounding the aggregates. The flow obtained for the mixtures under study presented very similar values and complied with the established requirements.

The durability of the asphalt surface layer is a function of the void content, given that the fewer voids, the lower its permeability. But a very low void content can cause exudation of the asphalt cement. The foregoing allows us to specify that the studied mixtures presented an adequate void content that guarantees good behavior. The voids with air in the mixtures presented similar values, 4.67%, 4.92%, and 4.99%, respectively. On the other hand, VMA values slightly increased in BFD mixtures by 15.80% in M-1, 17.36% in M-50, and 19.37% in M-100. The slight increase in this parameter can be attributed to the increase in the asphalt cement content in each mixture. This increase represents more available space to accommodate the effective volume of asphalt, which is favorable since the thicker the asphalt cement film that covers the aggregate particles, the more durable the mix will be. In addition, if VAM is too low, the mix may suffer durability and dry appearance problems, and if VAM is too high, the mix may present stability problems [21].

Table 4.
Values for the Marshall design for each mixture

Marshall Test	Unit	Value			Criteria
		M-0	M-50	M-100	
Asphalt content (by weight)	%	5.4	7.2	7.9	-
Specific gravity bulk (G_{mb})	g/cm^3	2.39	2.25	2.11	-
Stability	N	13500	12100	11200	9000
Flow	mm	3.35	3.21	3.16	2.0 – 3.5
Ratio: stability/flow	kN/mm	4.03	3.77	3.54	3.0 - 6.0
Voids with air (Av)	%	4.67	4.92	4.99	4.0 – 6.0
Voids in mineral aggregates (VAM)	%	15.80	17.36	19.37	>15.0
Asphalt-filled voids (VFA)	%	70.30	71.44	73.52	65 - 75

Source: the authors

Similarly, VFA values increased in BFD mixtures, 70.30%, 71.44%, and 73.52%, respectively. The higher VFA in BFD mixtures can be attributed to the chemical composition and its rough and porous microtexture. This can be beneficial for asphalt concrete since there will be greater adherence between the aggregate and the asphalt, resulting in greater durability.

3.1.2 Compaction indices

The compaction of an asphalt layer is important for its performance during its useful life, the level of compaction has a direct relationship with the air voids. A mix with high air content can have subsequent compaction due to vehicle loads and a mix with low air content can lead to problems such as exudation and premature deterioration of the asphalt layer [17].

The compaction graphs (number of gyrations Vs. % G_{mm}) prepared with the SGC data for the analyzed mixtures and the illustration of the CEI and TCI indices are shown in Figure 5 a and b.

The M-0 mix with the gyration number eight of the SGC reached 86.2% of G_{mm}, while the M-50 mix for the same number of gyrations reached 85.5% of G G_{mm}. Likewise, to reach 92% of G_{mm} (Av=8%), the M-0 mix needed 32 gyrations of SGC and the M-50 mix needed 42 gyrations, from which the CEI values for each mix result. In the case of TCI, the M-0 mix needed 95 gyrations to reach 96% of the G_{mm} (Av=4%) and the M-50 mix needed 104 gyrations. Likewise, the maximum density in the SGC, the M-0 mixture was obtained at 115 gyrations for a percentage of voids with air of 3.61% and the M-50 mixture with 120 gyrations, a percentage of voids of 3.51% was obtained, as illustrated in Fig. 5a.

On the other hand, the M-100 mix in gyration number eight reached 87.3% of the G_{mm}, while to reach 92% of the G_{mm} (Av=8%) it needed 37 gyrations, to reach 96% of the G_{mm} (Av=4 %), 105 gyrations were necessary, and at 125 gyrations the maximum density was obtained (Av=3.53%) as shown in Fig. 5b.

To determine the MSI and MRI indices, the compaction graphs (number of gyrations Vs. % Av) were prepared as seen in Fig. 6, which illustrates the concept of these indices. Fig. 6a shows the comparison of the indices of the base mix (M-0) and the M-50; in the same way, Fig. 6b illustrates the difference of the indices of the base mix (M-0) and the M-100.

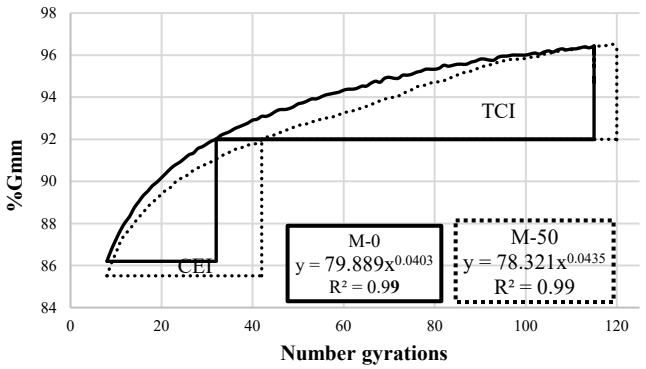

(a)

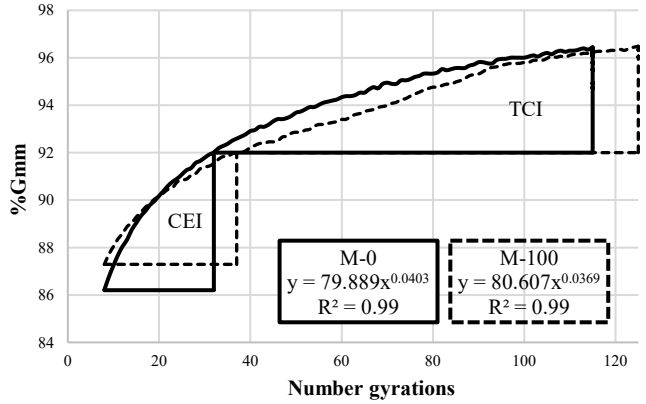

(b)

Figure 5. Compaction curves and comparison of CEI and TCI
Source: the authors.

Table 5 presents the numerical results of each index. A low CEI indicates a better workability in the mix, but a value that is too low means a tender mix that should be avoided [16] and higher CEI values indicate that they require more energy to be compacted during the construction process, that is, a greater number of roller passes. On the other hand, a high TCI is preferable in asphalt mixtures due to its ability to support more vehicle loads and prolong its useful life; it requires more compaction to achieve 4% voids with air [17]. An ideal asphalt mix would be one that has a low CEI and high TCI, which would be easier to compact during construction and difficult to compact under traffic loads.

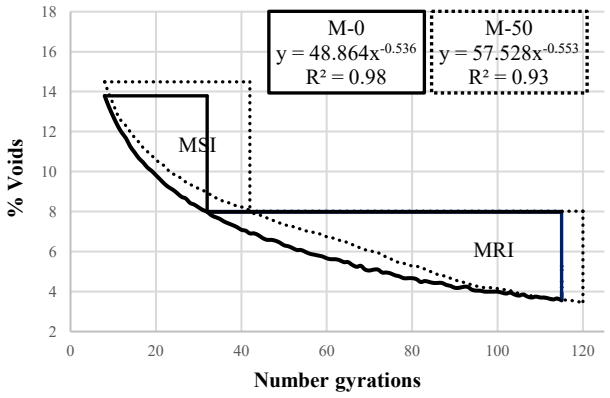

(a)

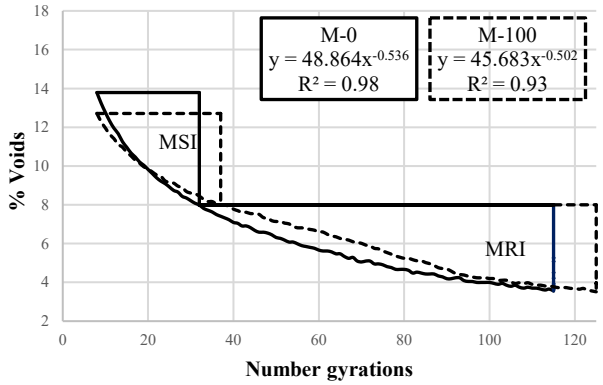

(b)

Figure 6. Compaction curves and comparison of MSI and MRI
Source: the authors.

In the same way, it is desirable that the MSI values are low, since this makes the mix more workable and easier to compact. On the other hand, it is recommended to have high MRI values, since this increases the resistance to compaction due to vehicle loads and provides adequate resistance to rutting [19].

Therefore, the ideal mixture would be the M-0 mixture since it presents the lowest CEI value and the highest TCI value. However, of the mixtures with the incorporation of BFD as an aggregate, the one that offers the best characteristics, according to the indices, is the M-100 mixture; which can be attributed to the presence of BFD as a fine aggregate, due to the greater affinity that this material has with asphalt cement. The M-50 mixture would require more compaction energy during its construction and would more easily reach 4% air voids due to compaction caused by traffic. In the same way, the results of MSI and MRI lead us to the same diagnosis.

Table 5.
Compaction index values

Índex	M-0	M-50	M-100
CEI: N=8; 92%G_{mm}	2246	3142	2707
TCI: 92%G_{mm}; 96%G_{mm}	6039	5936	6878
TCI: 92%G_{mm}; end. C.C.	7962	7473	7772
MSI: N=8; Av=8%	254	358	293
MRI: Av=8%; Av=4%	361	368	407
MRI: Av=8%; end. C.C.	438	426	427

Source: the authors

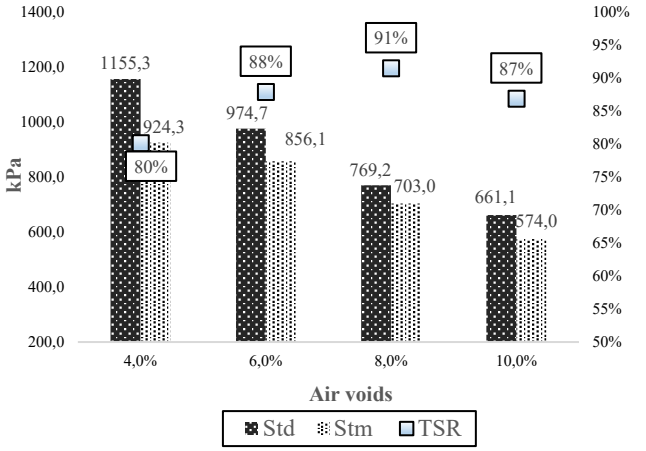

Figure 7. TSR results for mixture M-0
Source: the authors.

However, according to the compaction indices of the three mixtures analyzed, these do not present a considerable difference, which indicates that the compaction process, during construction and after putting the pavement into service, will have adequate behavior.

3.2 Moisture damage analysis

According to most specifications, the tensile strength ratio (TSR) must be greater than 80% to guarantee that the asphalt mix will not be further affected by the presence of water.

Fig. 7 shows the tensile strength values of the conditioned and unconditioned specimens, as well as the variation for each percentage of voids with air in the conventional M-0 mixture. As expected, the tensile strength of the conditioned specimens is lower than those obtained in the unconditioned ones, and the tensile strength decreases at a higher percentage of voids. However, the indirect TSR for all cases meets the minimum requirement of 80%, finding the highest value for 8% voids with air.

Fig. 8 shows the results of the mixture tensile strength test, where 50% of the fine aggregate was replaced by BFD (M-50). Similarly, the higher the void percentage, the greater the decrease in tensile strength in conditioned and unconditioned specimens. However, the variation is not as great as in the M-0 mix. Likewise, the TSR values in all cases meet the minimum defined requirement of 80%, although values higher than those shown in the M-1 mixture were found. Similarly, the highest TSR value occurs with 8% voids with air. This behavior can be attributed to the improved affinity between BFD and asphalt and the increased absorption percentage in BFD according to its texture and porosity.

On the other hand, an improvement is observed in the tensile strength of the conditioned specimens for 6.0%, 8.0% and 10.0% voids with air, to the values found in the M-0 mixture, as well as in the tensile strength of the unconditioned specimens for 8.0% and 10.0%. Thus, the partial substitution of the fine aggregate with BFD improves mix performance. These results can be attributed to the improved affinity of BFD, which forms a stronger bond with asphalt cement in the presence of water, which makes BFD a favorable material in the asphalt mix.

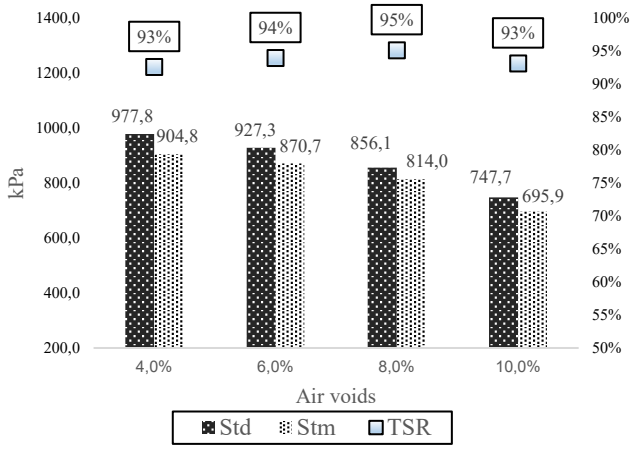

Figure 8. TSR results for mixture M-50
Source: the authors.

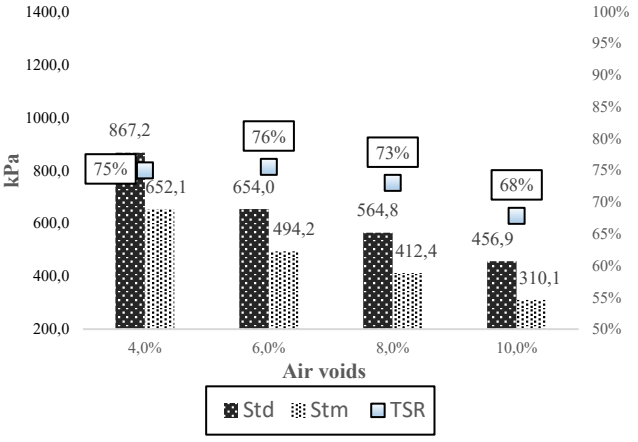

Figure 9. TSR results for mixture M-100
Source: the authors.

Fig. 9 shows M-100 performance. The tensile strength decreased considerably, compared to M-0 and M-50, both for the conditioned and unconditioned test pieces for all void percentages. In none of the cases is the minimum requirement of 80% in the TSR value met. The mixture with 100% BFD as fine aggregate did not show satisfactory resistance to moisture damage. The highest TSR value was found for 6.0% air voids, with a value of 76%. These results can be justified due to the higher content of asphalt cement, where the cohesive force of the asphalt is reduced, causing a decrease in mix rigidity [22,23].

The TSR of the designed mixtures and for each percentage of voids with air are shown in Fig. 10. The behavior of the base mix M-0 increases up to 8% voids with air; for 10% voids with air, the TSR value decreases by four percentage points regarding the value obtained for 8%. For the M-50 mix, there was an increase in the TRS values in all the percentages of voids with air compared to the base mix. However, in M-2, TSR behavior for the different percentages of voids with air is almost linear. It does not show great variation as the voids with air increase. The lowest TRS values were found in M-100 with decreases as the percentage of voids with air increases. The results of the tests indicate that using BFD aggregate in a percentage of up to 50% is favorable for the manufacture of asphalt mixes to be used as a wearing course.

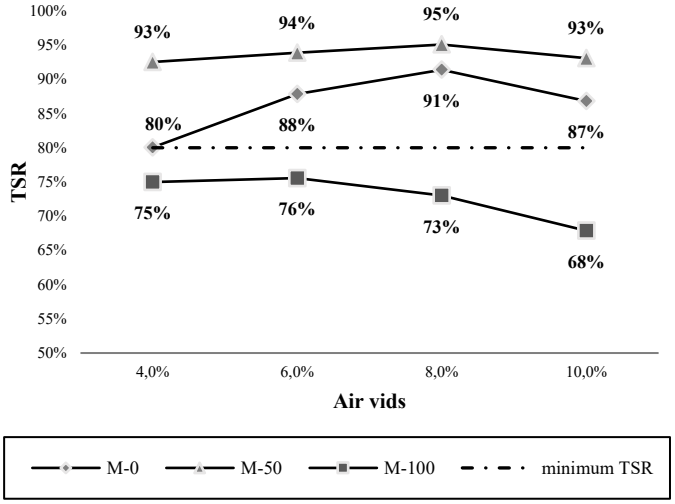

Figure 10. Influence of the BFD aggregate on the tensile strength ratio (TSR)
Source: the authors

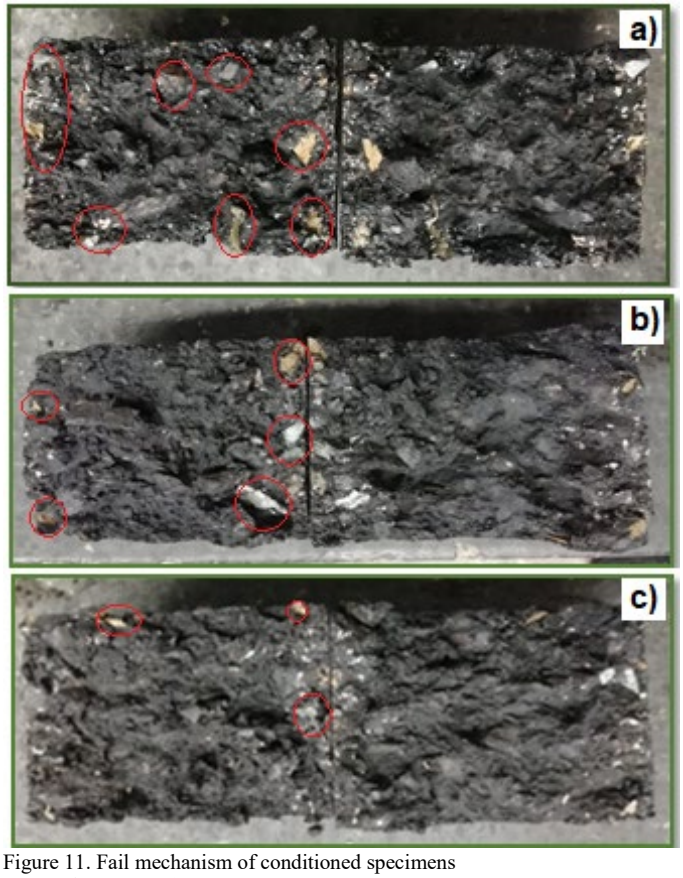

Figure 11. Fail mechanism of conditioned specimens
a) M-0, b) M-50 y c) M-100
Source: the authors.

The visual inspection of the tested specimens that presented the highest TSR value for each type of mixture indicated that the unconditioned specimens failed regarding the course aggregate rupture in all the mixtures studied, while the conditioned ones, for M-0, showed a failure surface due to loss of adhesion and weakening of the aggregate-asphalt union, Fig. 11a.

In the case of the conditioned test tubes of the M-50 mix, Fig. 11b, there was a smaller failure surface associated with a loss of adhesion between the aggregate and the asphalt and the greater failure surface was related to a reduction in asphalt cohesive force. Fig. 11c shows the conditioned specimen of the M-100 mix. There are few aggregates without an asphalt coating, which indicates that the failure due to adhesion loss decreased remarkably and the largest surface presents a black color, which indicates the loss in the cohesive strength of the asphalt [24][25].

4 Conclusions

After the analysis of the compaction indices using the Superpave gyratory compactor, it can be concluded that the results obtained indicate that there is no considerable difference in the three evaluated mixes, M-0, M-50, and M-100. This suggests that, in terms of compaction, all the mixtures meet the required standards and have a similar behavior in terms of their density and structure. However, it is important to consider that this result only refers to the compaction index and that other properties and characteristics of the mixtures may vary and should be evaluated separately.

To analyze the incidence of BFD, the fine aggregate was partially and totally replaced in the studied mixtures. The Marshall design determined that the optimum content of asphalt binder in mixtures with BFD is greater than the asphalt necessary to obtain the best characteristics in the M-0 mixture. The M-50 mix increased by only 1.8% compared to the base mix. Similarly, the M-100 mixture achieved an increase of 2.5%. These results are supported by the BFD's surface texture and higher absorption compared to sand.

The physical-mechanical behavior of the mixtures with partial and total fine aggregate replacement with BFD is acceptable. The mixes meet all the Marshall design parameters required in the specifications. Therefore, the incorporation of BFD in asphalt mixes for pavements does not impair their performance. On the contrary, it helps in the use of industrial waste, contributing to the environmental impact and the sustainable development of materials for pavements.

According to our results, BFD additions of up to 50% in asphalt mixtures improve the behavior against moisture damage in rolling layers for pavements. Tensile strength values increase. Therefore, the TSR values improve. The use of a higher BFD percentage would be possible by incorporating additives that improve asphalt cohesion.

The behavior of voids with air turned out as expected: as the void percentage increased, the mixtures showed greater damage to moisture. An optimal value of 8% voids with air is presented since it achieved the highest TSR values. However, when BFD totally replaced the fine aggregate, the mixture failed to meet the minimum recommended TSR.

Blast furnace dust (BFD), the material implemented in this research, offers optimal characteristics for use as fine aggregate in mixtures for asphalt concrete and increases aggregate-asphalt cohesion. A disadvantage in the use of this material is the increase in the asphalt cement content, which makes the mixtures more expensive, which can be compensated in the long run with greater durability and resistance to moisture damage.

The implementation of BFD as a fine aggregate in asphalt mixes contributes to having more environmentally friendly asphalt mixes considering that waste generated by the steel industry is repurposed, which would otherwise accumulate in storage yards, and the exploitation of non-renewable conventional aggregates is reduced.

Acknowledgements

The authors thank José Manuel Sierra, director of the laboratory of materials and pavements of the school of Transport and Road Engineering of the UPTC. also, to *INCITEMA* for the collaboration in carrying out the chemical characterization tests. To the companies: *Votorantin-Acerías Paz del Río S.A*, *Triturados Paz del Rio S.A.* and *Incoasfaltos S.A.S.*, for the supply of materials.

References

[1] Lobato, N.C.C., Villegas, E.A., and Mansur,M.B., Management of solid wastes from steelmaking and galvanizing processes: a brief review, Resour. Conserv. Recycl., 102, pp. 49–57, 2015. DOI: https://doi.org/10.1016/j.resconrec.2015.05.025.

[2] Hu,T., Sun,T., Kou, J., Geng, C., Wang, X., and Chen, C., Recovering titanium and iron by co-reduction roasting of seaside titanomagnetite and blast furnace dust, Int. J. Miner. Process., 165, pp. 28–33, 2017. DOI: https://doi.org/10.1016/j.minpro.2017.06.003.

[3] Reyes, F.A. y Figueroa, A.S., Análisis de la susceptibilidad al daño por humedad de una mezcla asfáltica a partir del ensayo mist y del programa ipas 2d ®, Rev. Infraestruct. Vial - LanammeUCR, 17, (2215–3705), pp. 31–39, 2016.

[4] Hernández, R., Limón, P., Sandoval, I. y Cremades, I., Análisis de la susceptibilidad a la humedad de varios tipos de mezclas asfálticas mediante el módulo dinámico, in Expo-Asfalto 2017.

[5] C. Instituto Nacional de Vías, Art. 410-13 Suministro de Cemento Asfáltico, Bogotá, 2022.

[6] INVIAS, Artículo 450-22 Mezclas asfálticas en caliente de gradación continua, Bogotá, 2022.

[7] Asmerican Society for Testing and Materials, ASTM D6927-15 Standard test method for Marshall stability and flow of asphalt mixtures, Philadelphia, [Online]. 2015. Available at: https://doi.org/10.1520/D6927-15.

[8] Kehagia, F., Skid resistance performance of asphalt wearing courses with electric arc furnace slag aggregates, Waste Manag. Res., 27, (3), pp. 288–294, 2009. DOI: https://doi.org/10.1177/0734242X08092025.

[9] Xie, J., Chen, J., Wu, S., Lin, J., and Wei, W., Performance characteristics of asphalt mixture with basic oxygen furnace slag, Constr. Build. Mater., 38, pp. 796–803, 2013. DOI: https://doi.org/10.1016/j.conbuildmat.2012.09.056.

[10] Sorlini, S., Sanzeni, A., and Rondi, L., Reuse of steel slag in bituminous paving mixtures, J. Hazard. Mater., (209–210), pp. 84–91, 2012. DOI: https://doi.org/10.1016/j.jhazmat.2011.12.066.

[11] Ameri, M., Hesami, S., and Goli, H., Laboratory evaluation of warm mix asphalt mixtures containing electric arc furnace (EAF) steel slag, Constr. Build. Mater., 49, pp. 611–617, 2013. DOI: https://doi.org/10.1016/j.conbuildmat.2013.08.034.

[12] Wang, G., Determination of the expansion force of coarse steel slag aggregate, Constr. Build. Mater., 24, (10), pp. 1961–1966, 2010. DOI: https://doi.org/10.1016/j.conbuildmat.2010.04.004.

[13] Chen, Z., Wu, S., Wen, J., Zhao, M., Yi, M., and Wan, J., Utilization of gneiss coarse aggregate and steel slag fine aggregate in asphalt mixture, Constr. Build. Mater., 93, pp. 911–918, 2015. DOI: https://doi.org/10.1016/j.conbuildmat.2015.05.070.
[14] Xie, J., Wu, S., Lin, J., Cai, J., Chen, Z., and Wei, W., Recycling of basic oxygen furnace slag in asphalt mixture: Material characterization & moisture damage investigation, Constr. Build. Mater., 36, pp. 467–474, 2012. DOI: https://doi.org/10.1016/j.conbuildmat.2012.06.023.
[15] Hesami, S., Ameri, M., Goli, H., and Akbari, A., Laboratory investigation of moisture susceptibility of warm-mix asphalt mixtures containing steel slag aggregates, Int. J. Pavement Eng., 16, (8), pp. 745–759, 2015. DOI: https://doi.org/10.1080/10298436.2014.953502.
[16] Fatin, A., and Mahmoud, F., Wisconsin highway research program using the gyratory compactor to measure mechanical stability of asphalt mixtures, October, 2004.
[17] Tedla, T.A., Singh, D., and Showkat, B., Effects of air voids on comprehensive laboratory performance of cold mix containing recycled asphalt pavement, Constr. Build. Mater., 368, (November), 2022, art. 130416, 2023. DOI: https://doi.org/10.1016/j.conbuildmat.2023.130416.
[18] Kim, Y., Im, S., and Lee, D.H., Impacts of curing time and moisture content on engineering properties of cold in-place recycling mixtures using foamed or emulsified asphalt, J. Mater. Civ. Eng., 23, (5), pp. 542–553, 2011. DOI: https://doi.org/10.1061/(ASCE)MT.1943-5533.0000209.
[19] Delrio-Prat, M., Vega-Zamanillo, A., Castro-Fresno, D., and Calzada-Pérez, M.Á., Energy consumption during compaction with a Gyratory Intensive Compactor Tester. Estimation models, Constr. Build. Mater., 25, (2), pp. 979–986, 2011. DOI: https://doi.org/10.1016/j.conbuildmat.2010.06.083.
[20] ASTM D 4867/D4867M, Standard Test Method for Effect of Moisture on Asphalt Concrete Paving Mixtures 1, Annu. B. Am. Soc. Test. Mater. ASTM Stand., pp. 1–5, 2006. DOI: https://doi.org/10.1520/D4867.
[21] Garnica, A.P., Flores, F.M., y Alamilla, D.H., Caracterización geomecánica de mezclas asfálticas, Inst. Mex. del Transp., (267), 2005, 105 P.
[22] Ling, C., Hanz A., and Bahia, H., Measuring moisture susceptibility of Cold Mix Asphalt with a modified boiling test based on digital imaging, Constr. Build. Mater., (105), pp. 391–399, 2016. DOI: https://doi.org/10.1016/j.conbuildmat.2015.12.093.
[23] Cucalon, L.G., Yin, F.A., Martin, E., Arambula, E., Estakhri, C., and Park, E.S., Evaluation of moisture susceptibility minimization strategies for warm-mix asphalt: case study, J. Mater. Civ. Eng., 28, (2,) 2016. DOI: https://doi.org/10.1061/(asce)mt.1943-5533.0001383.
[24] Figueroa, A.S., and Reyes, F.A., Influence of water in asphalt binders and its impact on stripping of asphalt mixtures, Mater. Sci. Eng., [Online]. 2012. Available at: https://www.semanticscholar.org/paper/A-5-EE-278-INFLUENCE-OF-WATER-IN-ASPHALT-BINDERS-ON-Figueroa-Reyes/f17e186e277650836e0ad14893b7610fd87694eb
[25] Chaturabong, P., and Bahia, H.U., Effect of moisture on the cohesion of asphalt mastic ond bonding with surface of aggregates, Road Mater. Pavement Des., 19, pp. 741–753, 2018. DOI: https://doi.org/10.1080/14680629.2016.1267659.

R. Ochoa-Díaz, is BSc. in Transportation and Roads Engineer and MSc. degree in Road Infrastructure, both from the Universidad Pedagógica y Tecnológica de Colombia, Tunja, Colombia. And PhD. in Engineering and Materials Science at the Universidad Pedagógica y Tecnológica de Colombia. He is professor with professional, academic and research experience in the area of pavements and new materials. He is active researcher of the road infrastructure research and development group, Grinfravial, at the School of Transportation and Roads Engineering the Universidad Pedagógica y Tecnológica de Colombia.
ORCID: 0000-0003-1151-7884

G.E. Grimaldo-León, is BSc. in Industrial Production Engineer from the Universidad Francisco de Paula Santander. MBA in Business Management from the Universidad Autónoma de Bucaramanga. She is research professor at the Universidad de Boyacá in the area of business management and researcher of the LOGyCA research group at the Universidad de Boyacá.
ORCID: 0000-0002-8211-4305

C.H. Higuera-Sandoval, is BSc. in Transportation and Roads Engineer and from the Universidad Pedagógica y Tecnológica de Colombia, Tunja, Colombia. And Master in Land Road Engineering from the Universidad del Cauca He is professor with professional, academic and research experience in the area of pavements. He is active researcher of the road infrastructure research and development group, Grinfravial, at the School of Transportation and Roads Engineering the Universidad Pedagógica y Tecnológica de Colombia.
ORCID: 0000-0003-1333-2517